crystals

MDPI

Article

Supramolecular Architecture in a Ni(II) Complex with a Weakly Bonded N,N′-(1,4-phenylenedicarbonyl)Diglycinate Counter-Anion: Crystal Structure Investigation and Hirshfeld Surface Analysis

Niels-Patrick Pook

Institute of Inorganic and Analytical Chemistry, Clausthal University of Technology, Paul-Ernst-Str. 4, D-38678 Clausthal-Zellerfeld, Germany; niels-patrick.pook@tu-clausthal.de; Tel.: +49-5323-72-2887

Received: 12 October 2019; Accepted: 21 November 2019; Published: 23 November 2019

Abstract: In this work, we describe the structural investigation of a Ni(II) complex, $[Ni(C_{12}H_8N_2)_2(H_2O)_2]_2 \cdot (C_{12}H_{10}N_2O_6) \cdot (NO_3)_2 \cdot 10H_2O$, with phenanthroline ligands, a deprotonated aromatic dicarboxylic acid, N,N′-(1,4-phenylenedicarbonyl)diglycine, and a nitrate as counter-anions, as well as water molecules. Noncovalent interactions, such as π–π stacking, lone-pair···π, and C–H···π between the phenanthrolines of the cationic complex, $[Ni(C_{12}H_8N_2)_2(H_2O)_2]^{2+}$, and counter-anions are observed. Moreover, the solvated and noncoordinating counter-anion, N,N′-(1,4-phenylenedicarbonyl)diglycinate, is embedded in classical and nonclassical hydrogen-bonding interactions with water molecules and phenanthrolines. The two water molecules coordinated by the Ni^{II} atom and hydrogen bonded to the carboxylate of the N,N′-(1,4-phenylenedicarbonyl)diglycinate show attractive secondary electrostatic interactions, and a DD/AA hydrogen bonding pattern is formed. The noncovalent interactions of the cationic complex and the solvated N,N′-(1,4-phenylenedicarbonyl)diglycinate counter anion were explored with a Hirshfeld surface analysis, and related contributions to crystal cohesion were determined. The results of the N,N′-(1,4-phenylenedicarbonyl)diglycinate counter anion were compared to those of a solvated N,N′-(1,4-phenylenedicarbonyl)diglycine molecule of a previously described copper(II) complex.

Keywords: crystal structure; nickel(II) complex; N,N′-(1,4-phenylenedicarbonyl)diglycine; phenanthroline ligand; supramolecular interactions; Hirshfeld surface analysis; π-stacking; hydrogen bonding; noncovalent interactions

1. Introduction

Since Alfred Werner published his theory of the constitution of inorganic compounds in 1893 [1,2], coordination compounds have attracted much attention. During this time period, the synthesis and structural investigation of these compounds have gained wide acceptance in material science because of their functional architectures and potential applications in catalysis [3–5], gas storage [6,7], and medicine [8,9], and as luminescent materials [10] or scintillators [11–13]. Today, we are able to test the performance of scintillators with a tabletop device [14,15]. This approach offers a great opportunity in the search for these materials and in closing the gap between organic and inorganic scintillators containing metals of d-block elements and aromatic ligands.

The framework of coordination complexes, including coordination polymers [16–19] of varying dimensions, is also composed of different noncovalent interactions and is, therefore, closely related to the field of supramolecular chemistry [20] and the process of self-assembly [21]. Trace elements of

nickel and cobalt as metal centers of the complexes of urease and vitamin B12 play an essential role in the biological enzymatic reactions of microorganisms, plants, and in the human metabolism [22–25]. The self-organization processes of these reactions are attributed to noncovalent interactions and are also responsible for the drug-delivery of biologically active agents [26], as well as the structural composition of DNA and RNA macromolecules [27]. In summary, the essential processes of biological and chemical systems are based on metal complexes and the steering forces of noncovalent interactions.

It is known from the literature that reactions of the aromatic diamino acid N,N′-(1,4-phenylenedicarbonyl)diglycine with d-block elements lead to interpenetrating networks of formed zigzag chains [28–32]. For our synthetic purpose, we offer the metal centers a bidentate complexing agent, such as bipyridine or phenanthroline, during their reactions with the N,N′-(1,4-phenylenedicarbonyl)diglycine. The electron-deficient bidentate nitrogen containing aromatic ligands has the ability to be involved in different π–π interactions [33,34]. Moreover, the goal is to block parts of the coordination sphere of the metal centers by using these ligands and to inhibit the forming of aforementioned zigzag chains.

As a result of the actual reactions, we have prepared two cobalt(II) complexes and a copper(II) complex, which contain bidentate bipyridine or bidentate phenanthroline ligands and N,N′-(1,4-phenylenedicarbonyl)diglycine molecules in the crystal structures [35–37]. In the built supramolecular networks, the embedded N,N′-(1,4-phenylenedicarbonyl)diglycine acts as the linking molecules between two cationic building blocks in an anionic or neutral form. The structural analysis of the copper(II) compound reveals an anionic monodentate bridging N,N′-(1,4-phenylenedicarbonyl)diglycinate and a neutral solvated N,N′-(1,4-phenylenedicarbonyl)-diglycine molecule in one crystal structure [37]. To further our study of the coordination behavior of the N,N′-(1,4-phenylenedicarbonyl)diglycine molecule with d-block elements in the presence of electron-deficient bidentate nitrogen containing aromatic heterocycles, and to discover scintillating coordination complexes and/or polymers, we prepared the present coordination compound (Scheme 1).

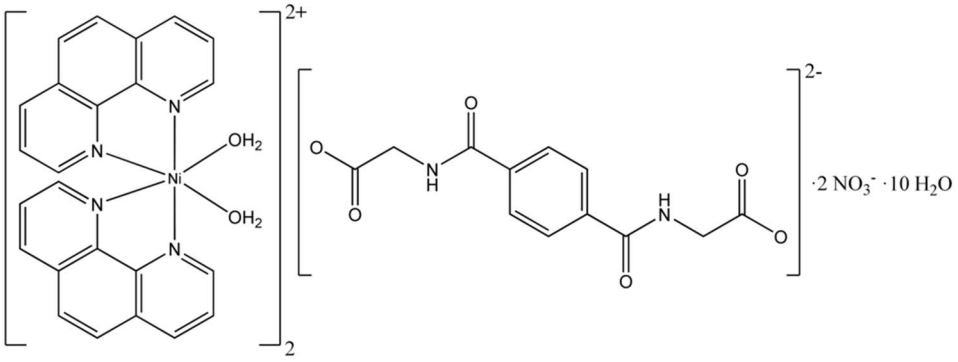

Scheme 1. Schematic representation of the Ni(II) coordination compound with phenanthroline ligands and the solvated N,N′-(1,4-phenylenedicarbonyl)diglycinate as a counter-anion.

Herein, the N,N′-(1,4-phenylenedicarbonyl)diglycine molecule is embedded in numerous noncovalent interactions and is a one of the main players of the constructed supramolecular network.

2. Experimental Section

2.1. Matrials and Synthesis of the N,N′-(1,4-Phenylenedicarbonyl)Diglycine

Nickel(II) nitrate hexahydrate (CAS 13478-00-7) was purchased from Merck KGaA (Darmstadt, Germany). The starting material, N,N′-(1,4-phenylenedicarbonyl)diglycine, was prepared according to the method of Cleaver and Pratt [38].

2.2. Preparation of the Ni(II) Complex

Cesium carbonate (2 mmol), N,N′-(1,4-phenylenedicarbonyl)diglycine (1 mmol), and 1,10-phenanthroline (2 mmol) were dissolved in a 1:1 (*v*/*v*) mixture of water and methanol (50 mL) and refluxed for 10 minutes. The mixture was allowed to cool to room temperature, and a previously prepared aqueous solution of nickel(II) nitrate (1 mmol) was slowly added under continuous stirring. After heating and cooling to room temperature, the formed pale green precipitate was filtered out. Pale-blue to violet block-shaped crystals of the complex were obtained by slow evaporation at room temperature within three days. Alternatively, a sodium salt of N,N′-(1,4-phenylenedicarbonyl)diglycine prepared from an aqueous solution of sodium hydroxide and N,N′-(1,4-phenylenedicarbonyl)diglycine in a stoichiometric ratio 2:1 could be used instead of cesium carbonate and N,N′-(1,4-phenylenedicarbonyl)diglycine. This route can also produce single crystals of a good quality suitable for X-ray crystallography.

2.3. X-ray Crystallography

Air-sensitive crystals of the nickel(II) coordination compound were separated from the mother liquor, and a well-shaped crystal was selected under a polarization microscope and sealed in a glass capillary with perfluorinated oil.

Intensity data sets were collected on a Stoe IPDS II diffractometer (Stoe, Darmstadt, Germany) using graphite monochromated MoK$_\alpha$ radiation (λ = 0.71073 Å). The SHELX-2018 [27] package was used for structure solution and refinement. The final structure solution was checked with PLATON [28]. The structure was solved by direct methods and refinement using the least-squares method on F^2 with the anisotropic displacement parameters for the non-H atoms. The crystal data and structure refinement parameters of the nickel(II) complex are listed in Table 1. All C-bound H atoms were set to idealized geometry and refined with Uiso(H) = 1.2 Ueq(C), C–H(aromatic) = 0.94 Å, and C–H(methylene) = 0.98 Å using a riding model. The water H atoms were located in a difference-Fourier map, and the isotropic displacement parameters were set to Uiso(H) = 1.5 Ueq(O). O2–H2A, O9—H9A/H9B, and O12—H12A/H12B were refined with O–H distances restrained to 0.82–0.87 Å, except for O13—H13A/H13B, which had a fixed distance of 1.009 Å and 0.973 Å, which led to a stable and consolidated hydrogen-bonding network. The nitrate anion was slightly disordered, and O6 could be split. Figures were prepared with DIAMOND [39] and POV-RAY [40]. Further details of the crystal structure investigation for the nickel(II) compound may be obtained free of charge from the Cambridge Crystallographic Data Centre (https://www.ccdc.cam.ac.uk/structures/) by quoting the deposition number CCDC 1957420.

Table 1. Crystal data and structure refinement parameters of the nickel(II) complex.

Compound	**$[Ni(C_{12}H_8N_2)_2(H_2O)_2]_2{\cdot}(C_{12}H_{10}N_2O_6){\cdot}(NO_3)_2{\cdot}10H_2O$**
Empirical formula	$C_{30}H_{35}N_6NiO_{13}$
Formula weight	746.35
Temperature (K)	223
Diffractometer	Stoe IPDS II
Wavelength (Å)	0.71073
Crystal system	triclinic
Space group	$P\bar{1}$ (No. 2)
a, *b*, *c* (Å)	12.5801(14), 12.5852(16), 12.6357(14)
α, *β*, *γ* (°)	114.670(9), 109.175(8), 95.749(10)
V (Å^3)	1650.2(4)
Z	2
D_{calc} (g·cm^3)	1.502
μ (mm^{-1})	0.664
F(000)	778
Crystal size (mm)	0.22 × 0.21 × 0.20
θ Range (°)	1.94–25.25

Table 1. *Cont.*

Compound	$[Ni(C_{12}H_8N_2)_2(H_2O)_2]_2{\cdot}(C_{12}H_{10}N_2O_6){\cdot}(NO_3)_2{\cdot}10H_2O$
Index ranges	$-15 \le h \le 15$ $-15 \le k \le 15$ $-15 \le l \le 15$
Reflection collected/unique	15380/5887
Completeness to θ (%)	98.5
Absorption correction	Numerical; X-AREA, X-RED (2008)
Max. and min. transmission	0.5023, 0.7193
Refinement method	Full-matrix least-squares on F^2
Data/parameters	5887/496
Goodness-of-fit on F^2	1.031
R_1 $[I \ge 2\sigma(I)]$/R_1 (all data)	0.0528/0.0615
wR_2 $[I \ge 2\sigma(I)]$/wR_2 (all data)	0.1406/0.1467
Largest diff. peak and hole (e·Å^3)	1.30, –0.58
Deposition number	CCDC 1957420

$R_1 = \sum||F_o| - |F_c|| / \sum|F_o|$; $wR_2 = \left[\sum w\left(F_o^2 - F_c^2\right)^2 / \sum w\left(F_o^2\right)^2\right]^{1/2}$; GOF $= \left[\sum w\left(F_o^2 - F_c^2\right)^2 / \left(n_{obs} - n_{param}\right)\right]^{1/2}$.

3. Results and Discussion

3.1. Description of the Crystal Structure

The complex cation of $[Ni(C_{12}H_8N_2)_2(H_2O)_2]_2{\cdot}(C_{12}H_{10}N_2O_6){\cdot}(NO_3)_2{\cdot}10H_2O$ contains two bidentate phenanthroline ligands and two water molecules, forming a distorted octahedral coordination sphere (Figures 1 and 2, and Table 2). A crystallographic center of inversion is located at the centroid of the noncoordinating and solvated N,N′-(1,4-phenylenedicarbonyl)diglycinate counter-anion. The asymmetric unit is completed by one noncoordinating nitrate counter-anion and five water molecules, which are involved in classical and nonclassical hydrogen-bonding. The hydrogen bond geometry is listed in Table 3. The distances and angles of the distorted octahedral coordination sphere of the Ni^{II} atom of the common cationic complex are similar to those found in the literature [41,42].

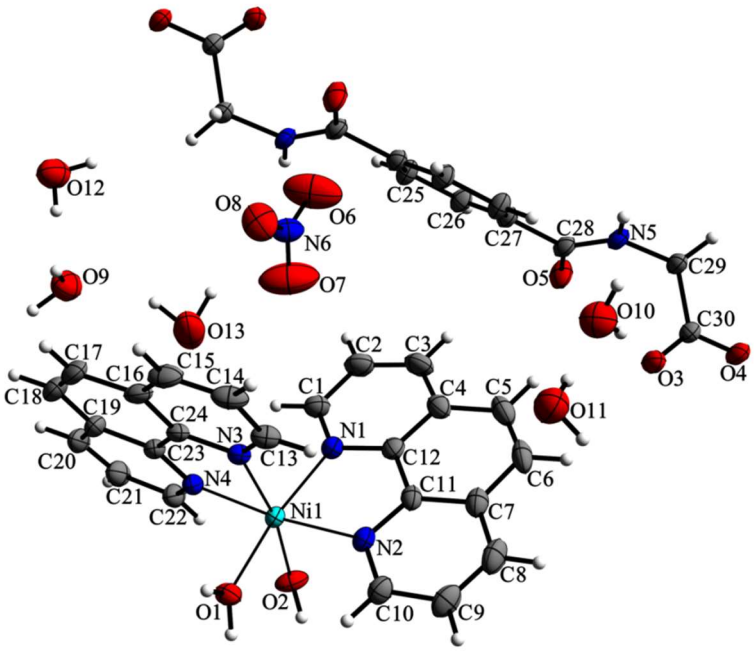

Figure 1. The molecular structure of the nickel(II) complex with the atomic numbering and displacement ellipsoids of non-H atoms drawn at a 40% probability level. Unlabeled atoms are related to labeled ones by the symmetry operation –x + 1, –y + 1, –z + 1 (see Tables 3 and 4 for details).

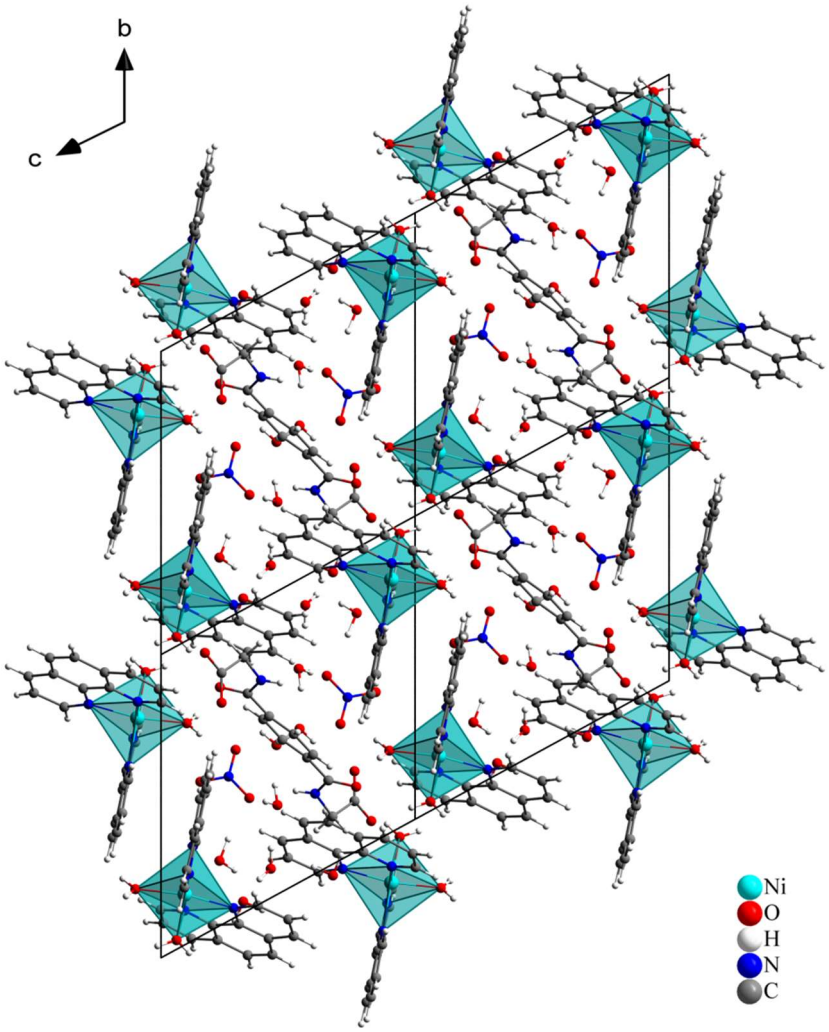

Figure 2. A view of the unit cells of $[Ni(C_{12}H_8N_2)_2(H_2O)_2]_2 \cdot (C_{12}H_{10}N_2O_6) \cdot (NO_3)_2 \cdot 10H_2O$ along the *a* axis with polyhedrons of the octahedral coordination sphere of $[Ni(C_{12}H_8N_2)_2(H_2O)]^{2+}$.

Table 2. Selected bond lengths (Å) and bond angle (°).

Bond	Lengths	Bond	Lengths
Ni–N1	2.095 (3)	Ni–N2	2.083 (3)
Ni–N3	2.101 (3)	Ni–N4	2.084 (3)
Ni–O1	2.088 (3)	Ni–O2	2.047 (2)
Bond	**Angle**	**Bond**	**Angle**
N1–Ni–N2	80.01 (11)	N2–Ni–N3	96.98 (11)
N3–Ni–N4	79.94 (11)	N4–Ni–N2	173.16 (11)
N1–Ni–N4	94.08 (12)	N1–Ni–N3	94.39 (12)
O1–Ni–N1	171.38 (11)	O1–Ni–N2	91.39 (11)
O1–Ni–N3	87.24 (10)	O1–Ni–N4	94.55 (11)
O2–Ni–N1	93.87 (3)	O2–Ni–N2	90.89 (12)
O2–Ni–N3	169.47 (9)	O2–Ni–N4	92.96 (12)
O1–Ni–O2	85.58 (10)		

Table 3. Hydrogen-bond geometry (Å, °).

D—H···*A*	*d*(*D*—H)	d(H···*A*)	*d*(*D*···*A*)	∠*D*—H···*A*
O1—H1*A*···O4^{iii}	0.87 (5)	1.82 (5)	2.692 (3)	175 (4)
O1—H1*B*···O5^{ii}	0.74 (5)	2.00 (5)	2.741 (3)	173 (4)
O2—H2*A*···O6^{iv}	0.84 (2)	1.91 (2)	2.739 (5)	166 (5)
O2—H2*A*···O7^{iv}	0.84 (2)	2.56 (4)	3.258 (6)	141 (4)
O2—H2*A*···N6^{iv}	0.84 (2)	2.57 (2)	3.389 (4)	166 (5)
O2—H2*B*···O3^{iii}	0.82 (5)	1.84 (5)	2.658 (3)	173 (5)
O9—H9*A*···O12^{xi}	0.79 (1)	2.05 (3)	2.787 (5)	154 (7)
O9—H9*B*···O4^{xv}	0.90 (2)	2.07 (3)	2.937 (4)	159 (6)
O10—H10*A*···O6^{i}	0.83 (7)	2.07 (7)	2.824 (6)	151 (7)
O10—H10*B*···O3	0.76 (8)	2.13 (8)	2.867 (5)	162 (7)
O11—H11*A*···O10	0.91 (8)	1.88 (8)	2.787 (6)	172 (7)
O11—H11*B*···O8^{v}	0.88 (8)	2.20 (8)	3.056 (6)	163 (7)
O11—H11*B*···N6^{v}	0.88 (8)	2.61 (8)	3.473 (5)	165 (6)
O12—H12*A*···O11	0.89 (2)	1.88 (2)	2.769 (5)	173 (7)
O12—H12*B*···O9^{v}	0.88 (2)	1.97 (2)	2.837 (5)	168 (7)
O13—H13*A*···O8	1.01 (2)	1.94 (3)	2.942 (6)	169 (8)
O13—H13*A*···N6	1.01 (2)	2.65 (4)	3.610 (6)	158 (7)
O13—H13*B*···O9	0.97 (2)	1.96 (5)	2.842 (6)	149 (8)
N5—H5···O8^{i}	0.85 (4)	2.07 (4)	2.900 (5)	164 (4)
C1—H1···O13	0.94	2.53	3.294 (5)	139
C2—H2···O7	0.94	2.55	3.469 (7)	166
C10—H10···O1	0.94	2.63	3.156 (4)	116
C13—H13···O12	0.94	2.54	3.415 (5)	156

Symmetry codes: (i) –x + 1, –y + 1, –z + 1; (ii) x, y + 1, z; (iii) –x, –y + 1, –z; (iv) –x + 1, –y + 1, –z; (v) x – 1, y, z; (xi) –x + 1, –y + 2, –z + 1; (xviii) x + 1, y + 1, z.

A SciFinder [43] search of the cationic complex yielded more than these two aforementioned references. We focused on these two structures due to the related chemical system. The nearly identical bond lengths of the carboxylate group in the solvated N,N′-(1,4-phenylenedicarbonyl)diglycinate counter-anion [C30—O4 = 1.256 (4) and C30—O2 = 1.244 (5) Å] indicate a delocalized bonding arrangement, rather than localized single and double bonds. The O3–C30–O4 angle of 126.1 (4) in the carboxylate group is slightly larger than that in the carboxylic group found in the copper complex [37]. In the noncoordinating N,N′-(1,4-phenylenedicarbonyl)diglycinate ligand, the deviations of atoms defining the central benzamido entity from its least-squares plane are −0.008 (4) Å (C28), 0.458 (3) Å (O5), −0.571 (3) Å (N5), and −0.671 (4) Å (C29). The angle between the amide group and the carboxylate group connected through the sp^3-hybridized methylene carbon atom (N5–C29–C30) is 115.0 (3)°. The dihedral angle between the planar carboxylate group (O3/C30/O4) and the aromatic synthon (C25–27/C25′–C27′) of the ligand is 65.7 (3)°, and thus much smaller than the value found in the copper complex [22]. The dihedral angle between the mean planes of the two bidentate phenanthroline ligands is 81.77 (5)°; the corresponding value between phenanthroline (N1/C1–C12/N2) and the coordinating water molecules (O1/Ni/O2) is 88.02 (8)°, and that between phenanthroline (N3/C13–C24/(N3/C13–C24/N4) and the coordinating water molecules is 88.97 (3)°.

A large number of different noncovalent interactions are present in the crystal structure (Figures 3–5). The nitrate anions are embedded in O–H···O, C–H···O and N–H···O hydrogen bonding with the water molecules, the phenanthroline ligands, and the solvated N,N′-(1,4-phenylenedicarbonyl)diglycinate counter anion (Figures 3 and 5). The two water molecules coordinated by the Ni^{II} atom and hydrogen bonded to the carboxylate show an attractive secondary electrostatic interaction [44,45] in the formed hydrogen-bonding pattern. The arrangement is similar to that found in the hydrogen bonded complex between the guanine and cytosine of nucleic acids [44,46]. The occurrence of an attractive diagonal interaction with a DD/AA motif [46,47] between the hydrogen bonded bridges supports the hydrogen bonding of the cationic complex and the N,N′-(1,4-phenylenedicarbonyl)diglycinate (Figures 3–5). The π–π

interactions between phenanthroline ligands stack these components along the different axes, showing a face-to-face arrangement (Figure 4). Centroid-to-centroid distances and explanations of the different centroids and their defining ring atoms are summarized in Table 4 and are similar to those in [48,49].

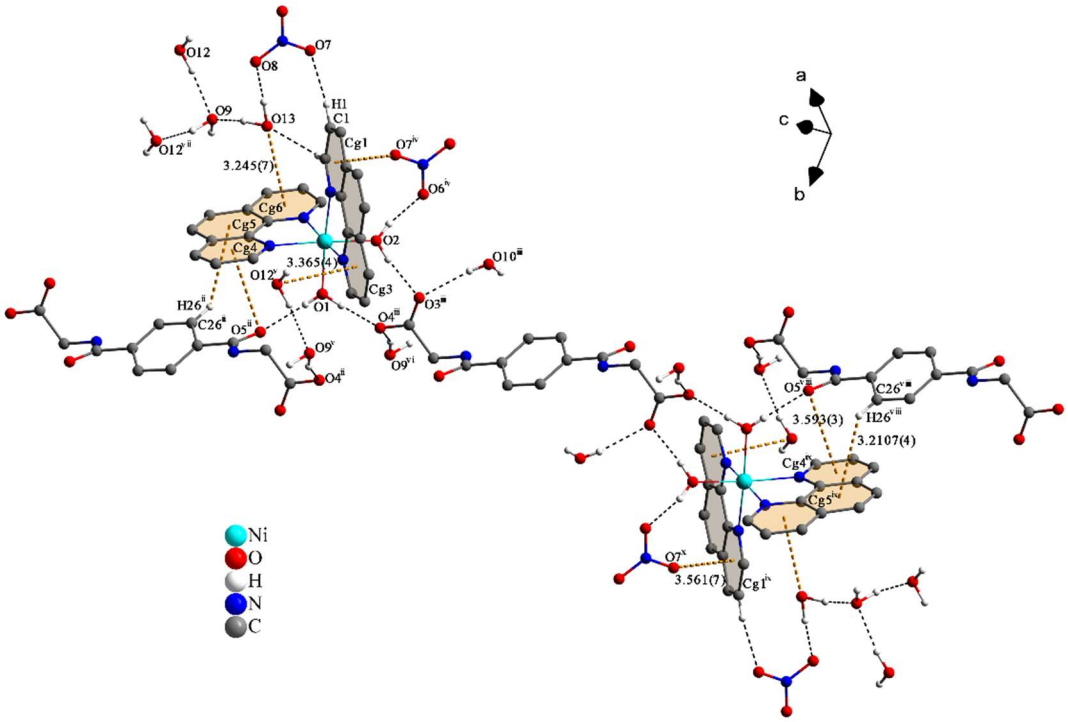

Figure 3. Different noncovalent interactions are present, such as classical hydrogen-bonding between water molecules, C–H···π interactions between aromatic moieties, and lone-pair···π interactions between the oxygen of the carboxylate groups or water molecules and the aromatic moieties. Hydrogen bonds are indicated by black dashed lines and π-interactions by yellow dashed lines. The hydrogen atoms not involved in interactions have been omitted for clarity. Distances are given in Å. Symmetry codes: (i) –x + 1, –y + 1, –z + 1; (ii) x, y + 1, z; (iii) –x, –y + 1, –z; (iv) –x + 1, –y + 1, –z; (v) x – 1, y, z; (vi) –x + 1, –y + 2, –z; (vii) –x + 2, –y + 2, –z + 1; (viii) –x – 1, –y, –z – 1; (ix) –x – 1, –y + 1, –z – 1; (x) x – 2, y, z – 1 (see Tables 3 and 4 for details).

Table 4. Parameters (Å, °) for C–H···π, lone-pair···π and π-π stacking interactions.

Y—X···Cg	d(X···Cg)	d(Y···Cg)	∠Y—X···Cg
C3—H3···Cg7	3.4215(5)	3.925(5)	115.9(3)
C8—H8···Cg1^{iii}	3.3517(7)	3.735(3)	106.9(3)
C15—H15···Cg1^{xi}	2.7372(5)	3.668(3)	170.3(3)
C26—H26···Cg5^{xv}	3.2107(4)	3.912(4)	132.9(2)
C28—O5···Cg4^{xv}	3.593(3)	3.581(4)	78.5(2)
N6—O7···Cg1^{iv}	3.561(7)	4.616(4)	147.3(4)
O12···Cg3^{xvi}	3.365(4)		
O13···Cg6	3.245(7)		
	Cg···Cg	**d(Cg···Cg)**	
	Cg2···Cg3^{iii}	3.6649(7)	
	Cg4···Cg4^{xi}	3.5600(4)	
	Cg6···Cg6^{vi}	3.5628(4)	

Cg1, Cg2, Cg3, Cg4, Cg5, Cg6, and Cg7 are the centroids defined by the ring atoms (N1/C1–C4/C12), (C4–C7/C11–C12), (N2/C7–C11), (N3/C13–C16/C24), (C16–C19/C23–24), (N4/C19–C23), and (C25–27/25′–27′), respectively. Symmetry codes: (iii) –x, –y + 1, –z; (iv) –x + 1, –y + 1, –z; (vi) –x + 1, –y + 2, –z; (xi) –x + 1, –y + 2, –z + 1; (xv) x, y – 1, z; (xvi) x + 1, y, z.

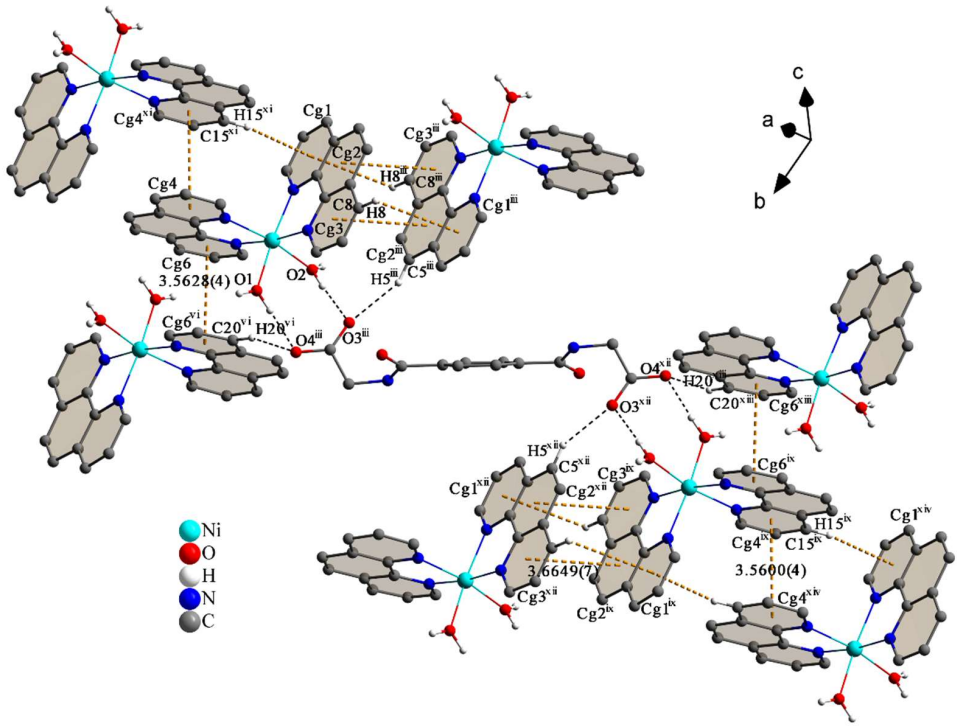

Figure 4. View of the C–H···O hydrogen-bonding between the aromatic moieties and oxygen atoms of the carboxylate groups, as well as the π–π stacking interactions between the complex cations. Noncovalent interactions are indicated by yellow dashed lines and C–H···O interactions by black dashed lines. The hydrogen atoms not involved in interactions have been omitted for clarity. Distances are given in Å. Symmetry codes: (iii) –x, –y + 1, –z; (vi) –x + 1, –y + 2, –z; (ix) –x – 1, –y + 1, –z – 1; (xi) –x + 1, –y + 2, –z + 1; (xii) x – 1, y, z – 1; (xiii) x – 2, y – 1, z – 1; (xiv) x – 2, y – 1, z – 2; (see Tables 3 and 4 for details).

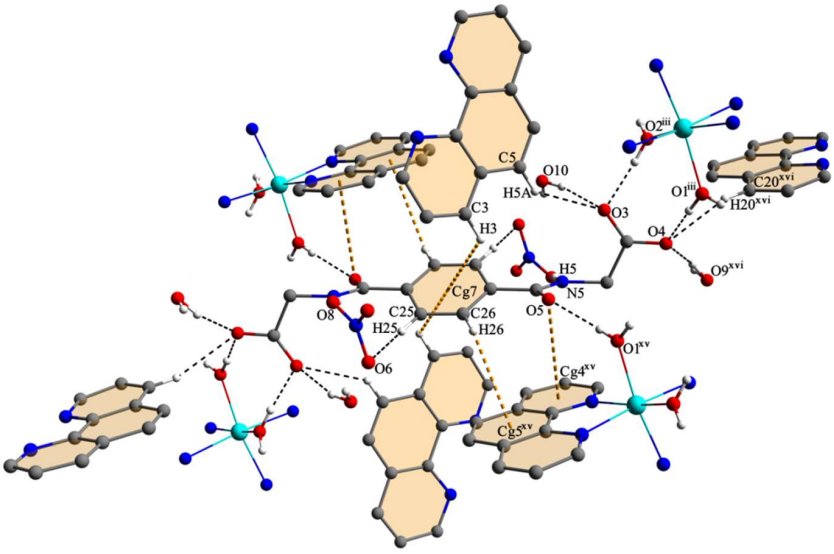

Figure 5. View of the extended network of noncovalent interactions with the embedded N,N′-(1,4-phenylenedicarbonyl)diglycinate and the adjacent phenanthrolines of the cationic complex. The O–H···O and C–H···O contacts are indicated by black dashed lines and different π-interactions by yellow dashed lines. Symmetry codes: (iii) –x, –y + 1, –z; (xv) x, y – 1, z; (xvi) x + 1, y, z (see Tables 3 and 4 for details).

Lone-pair···π interactions between the O5 atom of the carboxyl group of the noncoordinating N,N′-(1,4-phenylenedicarbonyl)diglycinate molecule and the Cg4 centroid of a phenanthroline ligand are observed. This value is similar to that found in the literature [50–53]. In addition, the lone-pair···π interactions of the two water molecules O12 and O13 with Cg3 and Cg6 of the phenanthrolines, respectively, and O7 of the nitrate counter-anion with the Cg1 of a phenanthroline ligand, are visualized in Figures 3 and 5. These distances are comparable with those found in related compounds [54–57]. Until very recently, lone-pair···π interactions were suggested to be directional. A Cambridge Structural Database (CSD) study [58] reveals that this is not always the case. Herein, it is concluded that only a small number (≤3%) of the molecules with lone-pairs are directly located over the center of the arene's surface, and this is caused as a side effect of the minimization of the volume in the crystal packing. From this point of view, the lone-pair···π interaction, as a supramolecular element for crystal engineering, can be discussed with a certain degree of skepticism. Finally, *C*–H···π interactions between the phenanthrolines and phenanthrolines and the noncoordinating N,N′-(1,4-phenylenedicarbonyl)diglycinate molecule of different arrangements are pictured in Figures 3–5 [59–61].

3.2. Hirshfeld Surface Analysis

The Hirshfeld surface (HS) [62,63] analysis was performed with Crystal Explorer [64,65] and the electrostatic potentials were calculated by using TONTO [66,67] with standard settings. All generated surfaces are represented transparently to facilitate visualization of the subjacent atoms and molecules. The HS is used to investigate the observed noncovalent interactions and substantiate the supramolecular assembly of the cationic complex (Figure 6) and noncoordinating N,N′-(1,4-phenylenedicarbonyl)diglycinate counter-anion (Figure 7) in the described crystal structure.

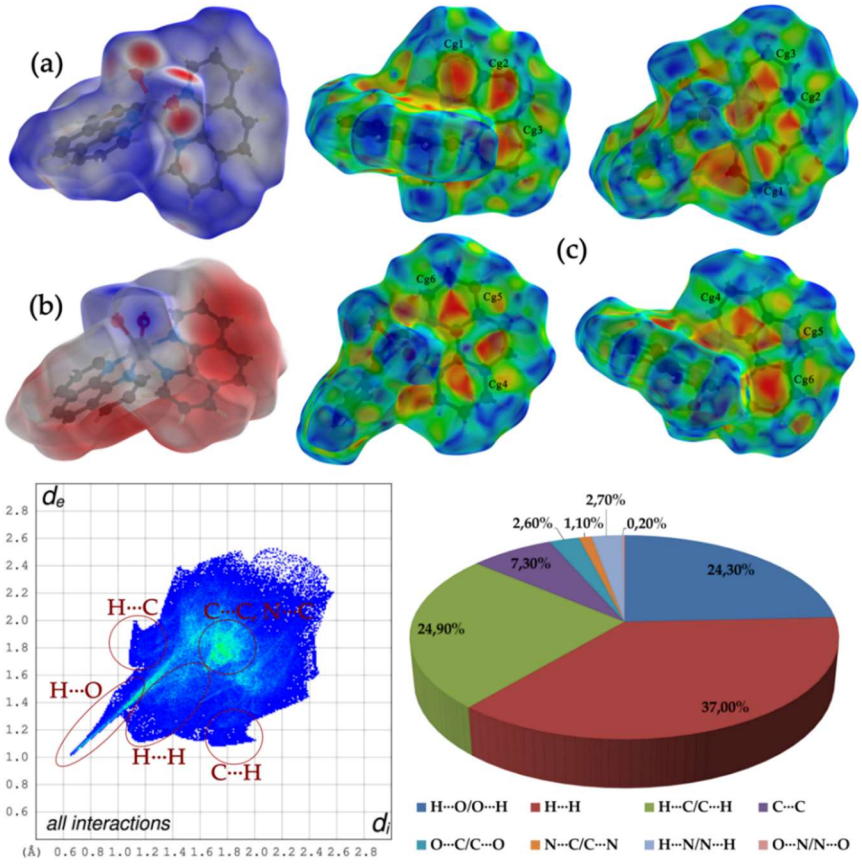

Figure 6. Hirshfeld surface (HS) analysis of the cationic complex over the d_{norm} (**a**), the electrostatic potential energy (**b**), and the shape index (**c**), with a 2D fingerprint plot for all interactions (**left**) and the percentage contribution to the HS (**right**).

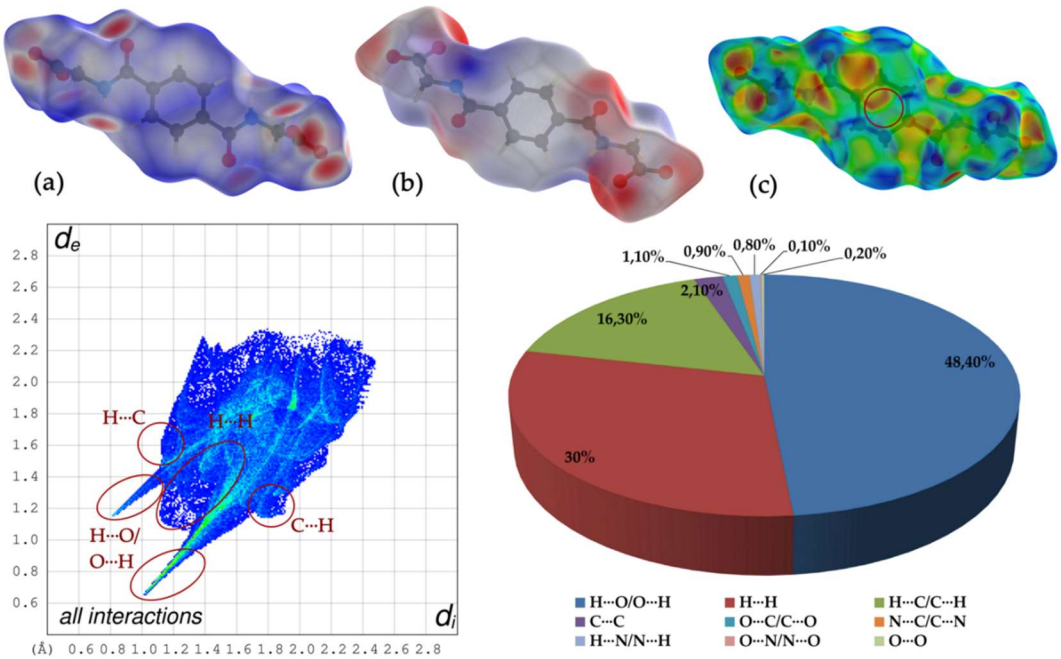

Figure 7. Hirshfeld surface analysis of the noncoordinating N,N′-(1,4-phenylenedicarbonyl)- diglycinate counter-anion over the d_{norm}: (**a**) the electrostatic potential energy (**b**) and the shape index (**c**) with a 2D fingerprint plot of all interactions (**left**) and the percentage contribution to the HS (**right**).

Two-dimensional fingerprint plots (FPs) of all interactions, and the percentage contributions to the HS of the different noncovalent interactions, are depicted in the figures. The internal d_i and external d_e distances between the HS and atom contacts are given in Å. The electrostatic potential energy and the d_{norm} of the HS of the cationic complex are plotted from –0.0472 to 0.2943 a.u. and from –0.7261 to 1.3002 a.u., respectively. The hydrogen-bonding interactions of the water molecules and some carbon-bonded hydrogens from the phenanthrolines of the cationic complex are indicated by the dark red spots of the HS mapped over the d_{norm} (**a**) and represent closer contacts than the van der Waals radii. The depiction of the HS mapped over the electrostatic potential (**b**) shows blue regions around the metal coordinating water molecules and some hydrogen atoms bonded to carbons of the phenanthrolines, thereby defining the positive electrostatic potential and identifying the hydrogen-bonded donor's aspects. This corresponds with the appearance of a large sharp single-spike in the FP of Figure 6 in the region of d_e ~ 1.02 Å /d_i ~ 0.67 Å and associated with classical and nonclassical hydrogen-bonding. The negative electrostatic potential of phenanthrolines is indicated by the red areas (**b**). The observations of the point-to-point arrangement of the red and blue triangles of the HS mapped over the shape index (**c**) reveal the face-to-face π–π stacking interactions of some aromatic moieties of the phenanthrolines, with a blue to green colored region around d_e ~ 1.80 Å /d_i ~ 1.80 of the C···C and N···C close contacts in the FP. Other red colored deformations of the HS with different shapes over some aromatic centers are attributed to the close contacts of oxygen atoms and hydrogen atoms according to lone-pair···π and C-H···π interactions. This is confirmed by the appearance of two symmetrical wings in the region of d_e ~ 1.66 Å /d_i ~ 1.10 Å and d_i ~ 1.62 Å /d_e ~ 1.12 Å of H···C/C···H in the FP. The main contributions of the cationic complex to the HS are assigned to the close contacts of H···H (37.0%), H···C/C···H (24.90%), H···O/O···H (24.30%), and C···C and N···C (adding to 8.40%), as shown in the pie chart of Figure 6.

For the noncoordinating N,N′-(1,4-phenylenedicarbonyl)diglycinate counter anion, the electrostatic potential energy and the d_{norm} are plotted in the range of –0.0869 to 0.1440 a.u. and –0.7269 to 1.3865 a.u., respectively, and are displayed in Figure 7. A multiplicity distances shorter than the van der Waals radii can be observed as dark red spots on the HS mapped over d_{norm} (**a**).

Thus, the carbonyl group and the hydrogen of the amide group, as well as the carboxylate group of the solvated N,N′-(1,4-phenylenedicarbonyl)diglycinate counter anion, are also involved in classical and nonclassical hydrogen bonding. The red regions of the HS mapped over the electrostatic potential (**b**) around the oxygen of the deprotonated carboxylate group and the carbonyl group of the amide are assigned to hydrogen-bond acceptors, in contrast to the blue region around the hydrogen atoms of the amide group, which can be assigned to the hydrogen-bonded donors. The two asymmetrical spikes in the regions of d_e ~ 1.66 Å /d_i ~ 1.10 Å and d_i ~ 1.62 Å /d_e ~ 1.12 Å of the H···O/O···H short contacts in the FP confirm this fact. The absence of red and blue triangles over the aromatic ring center of the solvated N,N′-(1,4-phenylenedicarbonyl)diglycinate in the HS, mapped over the shape index (**c**), indicate that the counter anion is not involved in π-π stacking interactions. A pair of asymmetrical wings of the H···C/C···H close contacts in the region of d_e ~ 1.59 Å /d_i ~ 1.15 Å and d_i ~ 1.72 Å /d_e ~ 1.15 Å in the FP suggest that the C–H···π interactions of N,N′-(1,4-phenylenedicarbonyl)diglycinate in the crystal and are visualized as a red colored deformation of the HS mapped over the shape index (**c**). The main contributions of N,N′-(1,4-phenylenedicarbonyl)diglycinate to the HS are assigned to the close contacts of H···O/O···H (48.40%), H···H (30.0%), and H···C/C···H (16.30), as shown in the pie chart of Figure 7. The large proportions of H···H close contacts of the cationic complex and the N,N′-(1,4-phenylenedicarbonyl)diglycinate counter anion (with values of 37% and 30%, respectively) are associated with the high number of hydrogen atoms in the structure. The main differences between the comparison of the present N,N′-(1,4-phenylenedicarbonyl)diglycinate counter anion and the N,N′-(1,4-phenylenedicarbonyl)diglycine solvent molecule of the previously-described Hirshfeld surface analyzed copper(II) complex [37] are the absence of C–C/C–N close contacts and a higher percentage contribution of H···C/C···H close contacts to the Hirshfeld surface. This is attributed to the involvement of π-stacking interactions of the N,N′-(1,4-phenylenedicarbonyl)diglycine solvent molecule of the copper(II) coordination compound and the C–H···π interactions of the N,N′-(1,4-phenylenedicarbonyl)diglycinate counter anion. Only a slight decrease of H···O/O···H close contacts of 6.2% (48.4% to 42.2%) could be observed. The H···H close contacts show no significant differences.

4. Conclusions

A Ni(II) complex, $[Ni(C_{12}H_8N_2)_2(H_2O)_2]_2{\cdot}(C_{12}H_{10}N_2O_6){\cdot}(NO_3)_2{\cdot}10H_2O$, with phenanthroline ligands and a deprotonated and noncoordinating solvated aromatic dicarboxylic acid, N,N′-(1,4-phenylenedicarbonyl)diglycine, has been synthesized. Air-sensitive crystals could be grown from aqueous solutions under ambient conditions, and this complex's structure was determined by single-crystal X-ray diffraction. In the present compound, the nickel ion exhibits a distorted octahedral coordination sphere defined by four nitrogen atoms of two bidentate phenanthroline ligands and two oxygen atoms of water molecules that construct a cationic complex $[Ni(C_{12}H_8N_2)_2(H_2O)_2]^{2+}$. The two water molecules coordinated by the Ni^{II} atom and hydrogen bonded to the carboxylate show attractive secondary electrostatic interactions. Thus, a DD/AA hydrogen-bonding pattern is formed. Finally, all aforementioned structurally determined compounds containing phenanthroline as electron-deficiency aromatic heterocycles and N,N′-(1,4-phenylene- dicarbonyl) diglycine in its ionic or neutral form reveal supramolecular assemblies varying in size and shape. Flexible and multifunctional N,N′-(1,4-phenylenedicarbonyl)diglycine molecules deserve further study of their coordination behavior with different d- and f-block elements in the search for scintillating and luminous materials.

Author Contributions: Experiments, structural refinement, and analysis, as well as Hirshfeld surface analysis, were designed and performed by the author. The author wrote the manuscript.

Funding: We acknowledge support by the Open Access Publishing Fund of Clausthal University of Technology.

Acknowledgments: The author is very indebted to A. Adam and M. Gjikaj for their support and helpful suggestions. The author thanks Joanna Richards Brauckmann and Raoul Brauckmann for proofreading (spelling and grammar).

Conflicts of Interest: The author declares no competing financial interests.

References

1. Werner, A. Beitrag zur Konstitution anorganischer Verbindungen. *Z. Anorg. Allg. Chem.* **1895**, *9*, 382–417. [CrossRef]
2. Constable, E.C.; Housecroft, C.E. Coordination chemistry: The scientific legacy of Alfred Werner. *Chem. Soc. Rev.* **2013**, *42*, 1429–1439. [CrossRef] [PubMed]
3. Scholl, M.; Ding, S.; Lee, C.W.; Grubbs, R.H. Synthesis and activity of a new generation of ruthenium-based olefin metathesis catalysts coordinated with 1,3-dimesityl-4,5-dihydroimidazol-2-ylidene ligands. *Org. Lett.* **1999**, *1*, 953–956. [CrossRef] [PubMed]
4. Ogba, O.M.; Warner, N.C.; O'Leary, D.J.; Grubbs, R.H. Recent advances in ruthenium-based olefin metathesis. *Chem. Soc. Rev.* **2018**, *47*, 4510–4544. [CrossRef] [PubMed]
5. Biefeld, C.G.; Eick, H.A.; Grubbs, R.H. Crystal structure of bis(triphenylphosphine)tetramethyleneplatinum(II). *Inorg. Chem.* **1973**, *12*, 2166–2170. [CrossRef]
6. Kitagawa, S.; Kitaura, R.; Noro, S.-I. Functional porous coordination polymers. *Angew. Chem. Int. Ed.* **2004**, *43*, 2334–2375. [CrossRef] [PubMed]
7. Li, H.; Wang, K.; Sun, Y.; Lollar, C.T.; Li, J.; Zhou, H.-C. Recent advances in gas storage and separation using metal-organic frameworks. *Mater. Today* **2018**, *21*, 108–121. [CrossRef]
8. Ndagi, U.; Mhlongo, N.; Soliman, M.E. Metal complexes in cancer therapy—An update from drug design perspective. *Drug Des. Dev. Ther.* **2017**, *11*, 599–616. [CrossRef]
9. Deo, K.M.; Ang, D.L.; McGhie, B.; Rajamanickam, A.; Dhiman, A.; Khoury, A.; Holland, J.; Bjelosevic, A.; Pages, B.; Gordon, C.; et al. Platinum coordination compounds with potent anticancer activity. *Coord. Chem. Rev.* **2018**, *375*, 148–163. [CrossRef]
10. Allendorf, M.D.; Foster, M.E.; Léonard, F.; Stavila, V.; Feng, P.L.; Doty, F.P.; Leong, K.; Ma, E.Y.; Johnston, S.R.; Talin, A.A. Guest-Induced Emergent Properties in Metal–Organic Frameworks. *J. Phys. Chem. Lett.* **2015**, *6*, 1182–1195. [CrossRef]
11. Allendorf, M.D.; Bauer, C.A.; Bhakta, R.K.; Houk, R.J.T. Luminescent metal-organic frameworks. *Chem. Soc. Rev.* **2009**, *38*, 1330–1352. [CrossRef] [PubMed]
12. Doty, F.P.; Bauer, C.A.; Skulan, A.J.; Grant, P.G.; Allendorf, M.D. Scintillating Metal-Organic Frameworks: A New Class of Radiation Detection Materials. *Adv. Mater.* **2009**, *21*, 95–101. [CrossRef]
13. Perry, J.J., IV; Feng, P.L.; Meek, S.T.; Leong, K.; Doty, F.P.; Allendorf, M.D. Connecting structure with function in metal-organic frameworks to design novel photo- and radioluminescent materials. *J. Mater. Chem.* **2012**, *22*, 10235. [CrossRef]
14. Pook, N.-P.; Fruhner, C.-J.; Franzl, T.; Denzer, U.; Adam, A. Instrumentation for X-ray Excited and Laser Induced Fluorescence Lifetime Spectroscopy Using Two-Dimensional Photon Counting. *IEEE Trans. Nuclear Sci.* **2012**, *59*, 2319–2323. [CrossRef]
15. Pook, N.-P.; Fruhner, C.-J.; Franzl, T.; Denzer, U.; Adam, A. Further performance tests of a picosecond X-ray and laser induced streak camera system with fast scintillation materials. *Radiat. Meas.* **2013**, *56*, 281–284. [CrossRef]
16. Batten, S.R.; Neville, S.M.; Turner, D.R. *Coordination Polymers*; Royal Society of Chemistry: Cambridge, UK, 2008; ISBN 978-0-85404-837-3.
17. Batten, S.R.; Champness, N.R.; Chen, X.-M.; Garcia-Martinez, J.; Kitagawa, S.; Öhrström, L.; O'Keeffe, M.; Paik Suh, M.; Reedijk, J. Terminology of metal–organic frameworks and coordination polymers (IUPAC Recommendations 2013). *Pure Appl. Chem.* **2013**, *85*, 1715–1724. [CrossRef]
18. Yamada, T.; Otsubo, K.; Makiura, R.; Kitagawa, H. Designer coordination polymers: Dimensional crossover architectures and proton conduction. *Chem. Soc. Rev.* **2013**, *42*, 6655–6669. [CrossRef]
19. Leong, W.L.; Vittal, J.J. One-Dimensional Coordination Polymers: Complexity and Diversity in Structures, Properties, and Applications. *Chem. Rev.* **2011**, *111*, 688–764. [CrossRef]
20. Schneider, H.-J. Binding Mechanisms in Supramolecular Complexes. *Angew. Chem. Int. Ed.* **2009**, *48*, 3924–3977. [CrossRef]

21. Cook, T.R.; Zheng, Y.-R.; Stang, P.J. Metal-Organic Frameworks and Self-Assembled Supramolecular Coordination Complexes: Comparing and Contrasting the Design, Synthesis, and Functionality of Metal-Organic Materials. *Chem. Rev.* **2013**, *113*, 734–777. [CrossRef]
22. Brenig, C.; Prieto, L.; Oetterli, R.; Zelder, F. A Nickel(II)-Containing Vitamin B12 Derivative with a Cofactor-F430-type π-System. *Angew. Chem. Int. Ed Engl.* **2018**, *57*, 16308–16312. [CrossRef] [PubMed]
23. Ragsdale, S.W. Nickel-based Enzyme Systems. *J. Biol. Chem.* **2009**, *284*, 18571–18575. [CrossRef] [PubMed]
24. Lawless, C.; Pearson, R.D.; Selley, J.N.; Smirnova, J.B.; Grant, C.M.; Ashe, M.P.; Pavitt, G.D.; Hubbard, S.J. Upstream sequence elements direct post-transcriptional regulation of gene expression under stress conditions in yeast. *BMC Genom.* **2009**, *10*, 7. [CrossRef] [PubMed]
25. Zambelli, B.; Musiani, F.; Benini, S.; Ciurli, S. Chemistry of Ni^{2+} in urease: Sensing, trafficking, and catalysis. *Acc. Chem. Res.* **2011**, *44*, 520–530. [CrossRef]
26. Meyer, E.A.; Castellano, R.K.; Diederich, F. Interactions with Aromatic Rings in Chemical and Biological Recognition. *Angew. Chem. Int. Ed.* **2003**, *42*, 1210–1250. [CrossRef]
27. Salonen, L.M.; Ellermann, M.; Diederich, F. Aromatic Rings in Chemical and Biological Recognition: Energetics and Structures. *Angew. Chem. Int. Ed.* **2011**, *50*, 4808–4842. [CrossRef]
28. Duan, J.; Zheng, B.; Bai, J.; Zhang, Q.; Zuo, C. Metal-dependent dimensionality in coordination polymers of a semi-rigid dicarboxylate ligand with additional amide groups: Syntheses, structures and luminescent properties. *Inorg. Chim. Acta* **2010**, *363*, 3172–3177. [CrossRef]
29. Kostakis, G.E.; Casella, L.; Hadjiliadis, N.; Monzani, E.; Kourkoumelis, N.; Plakatouras, J.C. Interpenetrated networks from a novel nanometer-sized pseudopeptidic ligand, bridging water, and transition metal ions with cds topology. *Chem. Commun.* **2005**, *30*, 3859–3861. [CrossRef]
30. Kostakis, G.E.; Casella, L.; Boudalis, A.K.; Monzani, E.; Plakatouras, J.C. Structural variation from 1D chains to 3D networks: A systematic study of coordination number effect on the construction of coordination polymers using the terepthaloylbisglycinate ligand. *New J. Chem.* **2011**, *35*, 1060–1071. [CrossRef]
31. Zhang, H.-T.; You, X.-Z. The one-dimensional zigzag coordination polymer catena -poly[[[triaquazinc(II)]-μ-N,N′-(benzene-1,4-dicarboxamido)diacetato-κ^2O:O′] dihydrate]. *Acta Crystallogr.* **2005**, *E61*, 1163–1165. [CrossRef]
32. Zhang, H.-T.; Li, Y.-Z.; Wang, T.-W.; Nfor, E.N.; Wang, H.-Q.; You, X.-Z. A ZnII-Based Chiral Crystalline Nanotube. *Eur. J. Inorg. Chem.* **2006**, *17*, 3532–3536. [CrossRef]
33. Janiak, C. A critical account on π–π stacking in metal complexes with aromatic nitrogen-containing ligands. *J. Chem. Soc. Dalton Trans.* **2000**, *21*, 3885–3896. [CrossRef]
34. Berryman, O.B.; Johnson, D.W. Experimental evidence for interactions between anions and electron-deficient aromatic rings. *Chem. Commun.* **2009**, *22*, 3143–3153. [CrossRef] [PubMed]
35. Pook, N.-P.; Gjikaj, M.; Adam, A. Bis[bis(2,2′-bipyridine-κ^2N,N′)(carbonato-κ^2O,O′)cobalt(III)] 2-{4-[(carboxylatomethyl)carbamoyl] benzamido}acetatehexahydrate. *Acta Crystallogr.* **2014**, *E70*, 160–161. [CrossRef]
36. Pook, N.-P.; Hentrich, P.; Gjikaj, M. Crystal structure of bis-tris-(1,10-phenanthroline-κ^2N,N′)cobalt(II) tetranitrate N,N′-(1,4-phenylenedicarbonyl)diglycine solvate octahydrate. *Acta Crystallogr.* **2015**, *E71*, 910–914. [CrossRef]
37. Pook, N.-P.; Adam, A.; Gjikaj, M. Crystal structure and Hirshfeld surface analysis of (μ-2-{4-(carboxyl-atometh-yl) carbamoylbenzamido}-acetato-κ^2O:O′)bis-bis-(1,10-phenanthroline-κ^2N,N′)-copper(II) dinitrate N,N′-(1,4-phenylenedicarbonyl)diglycine monosolvateoctahydrate. *Acta Crystallogr.* **2019**, *E75*, 667–674. [CrossRef]
38. Cleaver, C.S.; Pratt, B.C. Synthesis of 2,2′-Bis-[5(4H)-oxazolones]. *J. Am. Chem. Soc.* **1955**, *77*, 1544–1546. [CrossRef]
39. Sheldrick, G.M. Crystal structure refinement with SHELXL. *Acta Crystallogr.* **2015**, *C71*, 3–8. [CrossRef]
40. Spek, A.L. Structure validation in chemical crystallography. *Acta Crystallogr.* **2009**, *D65*, 148–155. [CrossRef]
41. Köse, D.A.; Zümreoglu-Karan, B.; Koşar, B.; Büyükgüngör, O. Diaquabis(phen)Ni(II) Complex with Vitamin B13 Counter-ions. *J. Chem. Crystallogr.* **2008**, *38*, 305–309. [CrossRef]
42. Prior, T.J.; Rujiwatra, A.; Chimupala, Y. $[Ni(1,10\text{-phenanthroline})_2(H_2O)_2](NO_3)_2$: A Simple Coordination Complex with a Remarkably Complicated Structure that Simplifies on Heating. *Crystals* **2011**, *1*, 178–194. [CrossRef]

43. SciFinder. Chemical Abstracts Service: Columbus, OH, 2010; A Substructure Search with Chemical Structure Editor. Available online: https://scifinder.cas.org (accessed on 2 November 2019).
44. Jorgensen, W.L.; Pranata, J. Importance of secondary interactions in triply hydrogen bonded complexes: Guanine-cytosine vs uracil-2,6-diaminopyridine. *J. Am. Chem. Soc.* **1990**, *112*, 2008–2010. [CrossRef]
45. Van der Lubbe, S.C.C.; Zaccaria, F.; Sun, X.; Guerra, C.F. Secondary Electrostatic Interaction Model Revised: Prediction Comes Mainly from Measuring Charge Accumulation in Hydrogen-Bonded Monomers. *J. Am. Chem. Soc.* **2019**, *141*, 4878–4885. [CrossRef] [PubMed]
46. Kawahara, S.-I.; Uchimaru, T. Secondary Interaction Contribution in Hydrogen-Bonded Complex: Theoretical Model Study in Hydrogen Fluoride Trimer. *J. Comput. Chem. Jpn.* **2004**, *3*, 41–48. [CrossRef]
47. Zimmerman, S.C.; Murray, T.J. Hydrogen bonded complexes with the AA·DD, AA·DDD, and AAA·DD motifs: The role of three centered (bifurcated) hydrogen bonding. *Tetrahedron Lett.* **1994**, *35*, 4077–4080. [CrossRef]
48. Barceló-Oliver, M.; Terrón, A.; García-Raso, A.; Lah, N.; Turel, I. Intermolecular C–H·π interactions in 1,5-diphenyl-3-(2-pyridyl)-2-pyrazoline. *Acta Crystallogr.* **2010**, *C66*, 313–316. [CrossRef]
49. Kumar Seth, S.; Dey, B.; Kar, T.; Mukhopadhyay, S. Experimental observation of supramolecular carbonyl–π/π–π/π–carbonyl assemblies of CuII complex of iminodiacetate and dipyridylamine. *J. Mol. Struct.* **2010**, *973*, 81–88. [CrossRef]
50. Egli, M.; Sarkhel, S. Lone Pair—Aromatic Interactions: To Stabilize or Not to Stabilize. *Acc. Chem. Res.* **2007**, *40*, 197–205. [CrossRef]
51. Gao, X.-L.; Lu, L.-P.; Zhu, M.-L. The crucial role of C–H ... O and C=O ... π interactions in the building of three-dimensional structures of dicarboxylic acid–biimidazole compounds. *Acta Crystallogr.* **2009**, *C65*, o123–o127. [CrossRef]
52. Mooibroek, T.J.; Gamez, P.; Reedijk, J. Lone pair–π interactions: A new supramolecular bond? *CrystEngComm* **2008**, *10*, 1501–1515. [CrossRef]
53. Wan, C.-Q.; Chen, X.-D.; Mak, T.C.W. Supramolecular frameworks assembled via intermolecular lone pair-aromatic interaction between carbonyl and pyridyl groups. *CrystEngComm* **2008**, *10*, 475–478. [CrossRef]
54. Jain, A.; Ramanathan, V.; Sankararamakrishnan, R. Lone pair π interactions between water oxygens and aromatic residues: Quantum chemical studies based on high-resolution protein structures and model compounds. *Protein Sci.* **2009**, *18*, 595–605. [CrossRef] [PubMed]
55. Manna, P.; Seth, S.K.; Das, A.; Hemming, J.; Prendergast, R.; Helliwell, M.; Choudhury, S.R.; Frontera, A.; Mukhopadhyay, S. Anion Induced Formation of Supramolecular Associations Involving Lone pair−π and Anion−π Interactions in Co(II) Malonate Complexes: Experimental Observations, Hirshfeld Surface Analyses and DFT Studies. *Inorg. Chem.* **2012**, *51*, 3557–3571. [CrossRef] [PubMed]
56. Schottel, B.L.; Chifotides, H.T.; Dunbar, K.R. Anion-π interactions. *Chem. Soc. Rev.* **2008**, *37*, 68–83. [CrossRef]
57. Gamez, P.; Mooibroek, T.J.; Teat, S.J.; Reedijk, J. Anion Binding Involving π-Acidic Heteroaromatic Rings. *Acc. Chem. Res.* **2007**, *40*, 435–444. [CrossRef]
58. Jia, C.; Miao, H.; Hay, B.P. Crystal Structure Evidence for the Directionality of Lone Pair−π interactions: Fact or Fiction? *Cryst. Growth Des.* **2019**, *19*, 6806–6821. [CrossRef]
59. Gathergood, N.; Scammells, P.J.; Fallon, G.D. Inter- and intramolecular C–H·π interactions in morphine bis(1-naphthoate). *Acta Crystallogr.* **2003**, *C59*, 485–487. [CrossRef]
60. Nishio, M. CH/π hydrogen bonds in crystals. *CrystEngComm* **2004**, *6*, 130. [CrossRef]
61. Plevin, M.J.; Bryce, D.L.; Boisbouvier, J. Direct detection of CH/π interactions in proteins. *Nat. Chem.* **2010**, *2*, 466–471. [CrossRef]
62. Hirshfeld, F.L. Bonded-atom fragments for describing molecular charge densities. *Theor. Chim. Acta* **1977**, *44*, 129–138. [CrossRef]
63. Spackman, M.A.; Jayatilaka, D. Hirshfeld surface analysis. *CrystEngComm* **2009**, *11*, 19–32. [CrossRef]
64. Wolff, S.K.; Grimwood, D.J.; McKinnon, J.J.; Jayatilaka, D.; Spackman, M.A. *Crystal Explorer 3.1*; University of Western Australia: Perth, Australia, 2007.
65. Turner, M.J.; McKinnon, J.J.; Wolff, S.K.; Grimwood, D.J.; Spackman, P.R.; Jayatilaka, D.; Spackman, M.A. *Crystal Explorer 17*; The University of Western Australia: Perth, Australia, 2017.

66. Spackman, M.A.; McKinnon, J.J.; Jayatilaka, D. Electrostatic potentials mapped on Hirshfeld surfaces provide direct insight into intermolecular interactions in crystals. *CrystEngComm* **2008**, *10*, 377–388. [CrossRef]
67. Jayatilaka, D.; Grimwood, D.J.; Lee, A.; Lemay, A.; Russel, A.J.; Taylor, C.; Wolff, S.K.; Cassam-Chenai, P.; Whitton, A. TONTO—A System for Computational Chemistry. Available online: http://hirshfeldsurface.net/ (accessed on 22 November 2019).